

Title	Contact photolithographic micropatterning for bistable nematic liquid crystal displays
Author(s)	Niitsuma, Jun-ichi; Yoneya, Makoto; Yokoyama, Hiroshi
Citation	Applied Physics Letters, 92(24): 241120-1-241120-3
Issue Date	2008-06-20
Type	Journal Article
Text version	publisher
URL	<a href="http://hdl.handle.net/10119/8536">http://hdl.handle.net/10119/8536</a>
Rights	Copyright 2008 American Institute of Physics. This article may be downloaded for personal use only. Any other use requires prior permission of the author and the American Institute of Physics. The following article appeared in Jun-ichi Niitsuma, Makoto Yoneya, Hiroshi Yokoyama, Applied Physics Letters, 92(24), 241120 (2008) and may be found at <a href="http://link.aip.org/link/?APPLAB/92/241120/1">http://link.aip.org/link/?APPLAB/92/241120/1</a>
Description	

## Contact photolithographic micropatterning for bistable nematic liquid crystal displays

Jun-ichi Niitsuma,<sup>1,a)</sup> Makoto Yoneya,<sup>1,2</sup> and Hiroshi Yokoyama<sup>1,2</sup>

<sup>1</sup>Liquid Crystal Nano-System Project, ERATO/SORST, Japan Science and Technology Agency, 5-9-9 Tokodai, Tsukuba 300-2635, Japan

<sup>2</sup>Nanotechnology Research Institute, National Institute of Advanced Industrial Science and Technology (AIST), 1-1-1 Umezono, Tsukuba 305-8568, Japan

(Received 7 April 2008; accepted 24 May 2008; published online 20 June 2008)

Orthogonal alignment patterns of  $2 \times 2 \mu\text{m}^2$  size that induce nematic bistability were fabricated over  $4 \times 4 \text{cm}^2$  by a double exposure process employing a rewritable photoalignment material. Bistable liquid crystal cells with patterned surfaces were fabricated, and reproducible switching between the bistable states driven by orthogonal in-plane electric fields at 8.2 and 3.9 V/ $\mu\text{m}$  was confirmed. © 2008 American Institute of Physics. [DOI: 10.1063/1.2945631]

Surface bistable liquid crystal (LC) displays<sup>1</sup> with micropatterning have recently attracted increasing attention because of their reduced power consumption. Bistability can be achieved by using an alignment pattern in which the neighboring squares have orthogonal orientations [Fig. 1(a)], inducing the macroscopic bistable anchoring directions along the two diagonals.

To achieve this alignment, scanning-probe-based nanorubbing<sup>1,2</sup> and local oxidation<sup>3,4</sup> have been used. Alignment bistability<sup>1</sup> and even tristability<sup>2</sup> have been successfully demonstrated. These probe-based techniques are useful for proving the concept, but suffer from the slow throughput, rendering the technique impractical in industrial applications.

Photoalignment<sup>5-7</sup> is a promising approach to alleviating the problem of low throughput. Unlike the rubbing technique, photoalignment is a noncontact method that is based on the anisotropic photochemical reactions in the alignment layer induced by linearly polarized ultraviolet (LPUV) light, wherein the alignment direction is controlled by the polarization direction. In this method, dust and charge generation, which are the major drawbacks of conventional rubbing, can also be avoided. Lee and Kim<sup>8,9</sup> reported the fabrication of bistable photoaligned micropatterns using interfering laser light. However, the largest area treatable by this technique is limited to the coherent illumination area, and the spatial uniformity of light intensity is difficult to achieve. In contrast, contact photolithography permits instantaneous and uniform processing of large surface areas, making it a more attractive alternative for practical application.

The most important factor governing the resolution is the photomask-substrate gap. Figure 2 shows the simulated time-averaged spatial intensity profiles of LPUV light passing through the contact mask with various gaps. The calculations were performed for LPUV light with  $\lambda=365 \text{ nm}$  and a  $2 \times 2 \mu\text{m}^2$  checker pattern using a finite-difference time-domain method (FullWAVE,<sup>10</sup> RSoft Design Group, Inc.). Figure 2 shows that checker features are well preserved for gaps  $<750 \text{ nm}$ , while the field patterns become blurred and rounded for gaps  $>750 \text{ nm}$ . Realizing a gap  $<750 \text{ nm}$  over a large area likely will be the most serious challenge encountered in large-area contact photolithography.

In this study, we used LPUV light,  $\lambda=365 \text{ nm}$ , and the azo-based photoalignment material<sup>11</sup> described below. LPUV light irradiation at normal incidence to the azo film induces trans-cis isomerization of the azo group, which causes planar LC alignment in the direction perpendicular to the LPUV polarization direction.<sup>11</sup> Because of the reversibility of the isomerization, the alignment direction of the azo layer can be selectively rewritten in selected areas by a subsequent second LPUV exposure with different polarizations. By exploiting the rewritability of the azo material, the microchecker pattern shown in Fig. 1(a) can be fabricated without multiple photolithography. First, the entire azo layer is exposed to generate uniform alignment. Next, the same azo layer is exposed, through the microchecker photomask [Fig. 1(b)], to LPUV light polarized perpendicular to that of the first exposure. To ensure a small mask-substrate gap over the entire area, vacuum hard contact was used. A typical gap distance achieved with this method was  $<500 \text{ nm}$ . The key advantage

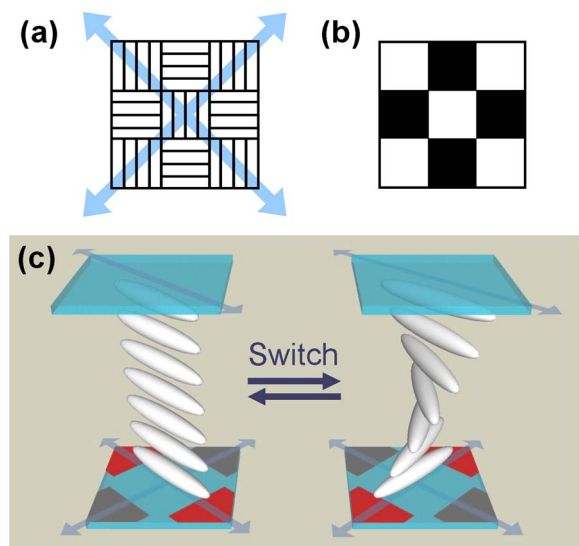


FIG. 1. (Color online) (a) Alignment pattern for a bistable surface on which neighboring squares are orthogonally aligned. Arrows indicate macroscopic bistable directions. (b) Pattern of checker photomask used to fabricate (a). (c) Schematic diagram of the bistable cell structure. The bottom substrate is micropatterned and the top substrate is uniformly aligned. The bistable states are HP (left) and TP (right). Pairs of electrodes used for switching are highlighted on the bottom.

<sup>a)</sup> Author to whom correspondence should be addressed. Electronic mail: niitsuma@nanolc.jst.go.jp.

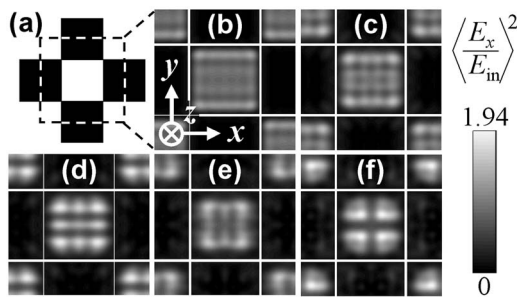


FIG. 2. Simulated time-averaged spatial intensity profiles of the electric fields transmitted through a checker photomask (a) consisting of squares of  $2 \times 2 \mu\text{m}^2$  at gap distances of (b)  $0.25 \mu\text{m}$ , (c)  $0.5 \mu\text{m}$ , (d)  $0.75 \mu\text{m}$ , (e)  $1 \mu\text{m}$  and (f)  $1.25 \mu\text{m}$ . The incident light with  $\lambda = 365 \text{ nm}$  is polarized along the  $x$  axis and travels along the  $z$  axis. The degree of depolarization of the transmitted light is  $<0.1$ . White lines indicate checker boundaries.

of the above photolithography process over multiple photolithography is that the new process does not require photomask positioning.

The photoalignment material we used was a polyamic acid with azobenzene units.<sup>12</sup> A 1 wt % solution of the azo polymer dissolved in *N*-methyl-2-pyrrolidone was spun onto a glass substrate and soft baked at  $70^\circ\text{C}$  for 30 min. The light from a Hg-Xe lamp (Ushio) was transmitted through Brewster polarizers followed by a bandpass filter ( $\lambda = 365 \pm 10 \text{ nm}$ ) and an integrator lens that homogenizes the intensity throughout the beam. The irradiation energy was  $2.1 \text{ mW/cm}^2$  over an area of  $\sim 30 \times 30 \text{ cm}^2$ . First and second exposure times were 15 and 20 min, respectively.

The bistable LC cell consisted of a checker-patterned substrate at the bottom and a unidirectional alignment substrate at the top. The top substrate, prepared by uniformly exposing the azo film to LPUV light, was oriented with respect to the bottom substrate in such a way that bistability between homogeneous planar (HP) and twisted planar (TP) configurations should result, as shown in Fig. 1(c). The cell with a gap of  $10 \mu\text{m}$  was filled with 4-*n*-pentyl-4'-cyanobiphenyl LC (5CB) in the isotropic phase. Switching between the bistable states was achieved by applying orthogonal in-plane electric fields with planar quadrupole electrodes on the bottom substrate at  $25^\circ\text{C}$ . After a rectangular ac voltage of 1 kHz frequency was applied to the opposing electrode pair, the field-off state was observed with a polarizing optical microscope at the same temperature.

Photographic images of a bistable cell with the patterned area of  $4 \times 4 \text{ cm}^2$  between polarizers are shown in Figs. 3(a) and 3(b). Most of the area was in the HP state, and spots of the TP state, which has a higher elastic energy due to LC twist deformation, with opposite brightness can be seen. The uniform bright or dark features of the HP state indicate uniform patterning over the entire area, confirming effective patterning. Figures 3(c)–3(e) show optical micrographs of the HP state for different polarizer arrangements. A square lattice with distinct boundaries was observed between crossed polarizers [Fig. 3(c)]. The checker pattern appeared for a  $45^\circ$  crossed polarizer arrangement [Fig. 3(d)], and the pattern was uniformly bright under parallel polarizers [Fig. 3(e)]. These results show that neighboring squares have orthogonal alignment directions, as depicted in Fig. 1(a).

Figure 4 shows the switching behavior of a bistable cell. The observation area was the central region surrounded by

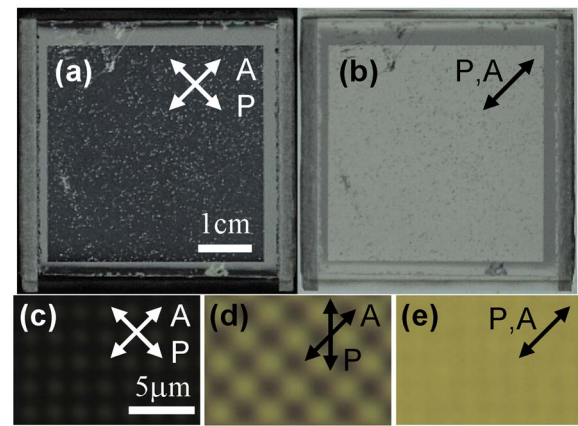


FIG. 3. (Color online) Images of a bistable LC cell observed between (a) crossed and (b) parallel polarizers. The arrows of P and A indicate polarizer and analyzer directions, respectively. The patterned area of  $4 \times 4 \text{ cm}^2$  (the innermost squares) is mainly in the HP state with spots in the TP state. [(c)–(e)] Optical micrographs of HP state with different polarizer orientations.

quadrupole electrodes. The HP  $\rightarrow$  TP switching started at  $8.2 \text{ V}_{\text{rms}}/\mu\text{m}$ , and switching of the entire region was complete at  $9.1 \text{ V}_{\text{rms}}/\mu\text{m}$ . (The electric field strength was defined as the root mean square of the applied voltage divided by the electrode separation of  $300 \mu\text{m}$ .) On the other hand, TP  $\rightarrow$  HP switching began at a fairly low voltage of  $3.9 \text{ V}_{\text{rms}}/\mu\text{m}$  and completed at  $5.3 \text{ V}_{\text{rms}}/\mu\text{m}$ . The switched state was maintained in the absence of electric field for at least three months in the dark. The switching field strengths are comparable to reported values,<sup>1,8,9</sup> but are not equal for HP  $\rightarrow$  TP and TP  $\rightarrow$  HP. The difference in the elastic energies of the two states has a negligible effect on the switching field because the twist energy of the TP state is four orders of magnitude smaller than the switching field energy. In order to understand the origin of the difference, one should recall that the checker pattern consists of two different subdomains. Two switching paths exist between HP and TP, depending on which subdomain undergoes orientation buckling, i.e.,  $\pi$ -rotation of the surface director.<sup>1</sup> The selection of the actual switching domain is dictated by the relative orientation of the electric field and the macroscopic alignment, so it becomes

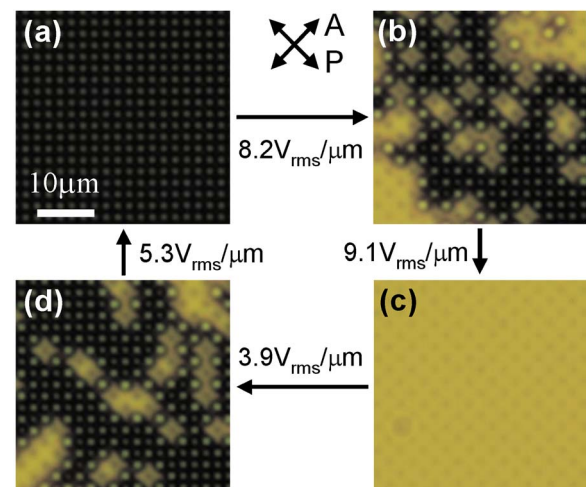


FIG. 4. (Color online) Polarized optical micrographs of switching of a bistable cell. (a) HP, (b) HP  $\rightarrow$  TP, (c) TP and (d) TP  $\rightarrow$  HP. The switching field was  $8.2 \text{ V}_{\text{rms}}/\mu\text{m}$  for HP  $\rightarrow$  TP and  $3.9 \text{ V}_{\text{rms}}/\mu\text{m}$  for TP  $\rightarrow$  HP, respectively.

very sensitive to the relative configuration of the electrodes and the micropattern. We believe that in the present cell, the HP→TP switching and the TP→HP switching are driven by the orientation buckling taking place on the different subdomains, thereby causing the threshold voltage difference that reflects the difference in the anchoring strengths on each respective subdomain.

We estimated the anchoring energy  $W_0$  of the photoaligned azo layer from the relation  $W_0 = 2E_{sw}\sqrt{\Delta\epsilon K_{22}}$ ,<sup>1</sup> where  $E_{sw}$  is the switching field strength,  $\Delta\epsilon$  is the dielectric anisotropy [ $7 \times 10^{-11}$  F/m (Ref. 13)] and  $K_{22}$  is the twist elastic constant [ $2 \times 10^{-12}$  N (Ref. 14)] of 5CB. With  $E_{sw} = 8.2$  V<sub>rms</sub>/μm and  $E_{sw} = 3.9$  V<sub>rms</sub>/μm for forward and backward switching, we find that  $W_0 = 2 \times 10^{-4}$  J/m<sup>2</sup> and  $W_0 = 1 \times 10^{-4}$  J/m<sup>2</sup> for respective subdomains.

In summary, we have fabricated microchecker patterns over an area of  $4 \times 4$  cm<sup>2</sup> by hard-contact photolithography using a rewritable azo photoalignment material. We demonstrated switching of the bistable cell in applied electric fields and obtained an anchoring energy of  $\sim 2 \times 10^{-4}$  J/m<sup>2</sup>. The single-mask photolithographic technique offers a simple and versatile route for fabricating large-area micropatterns that are difficult to realize by other patterning techniques. We hope that this method opens the way to the application of patterned alignment to novel LC devices.

The authors thank the referee for careful reading of the manuscript. J.N. thanks Dr. Y. Mitsuhashi for his continuous support and encouragement.

- <sup>1</sup>J.-H. Kim, M. Yoneya, J. Yamamoto, and H. Yokoyama, *Appl. Phys. Lett.* **78**, 3055 (2001).
- <sup>2</sup>J.-H. Kim, M. Yoneya, and H. Yokoyama, *Nature (London)* **420**, 159 (2002).
- <sup>3</sup>B. Zhang, F. K. Lee, O. K. C. Tsui, and P. Sheng, *Phys. Rev. Lett.* **91**, 215501 (2003).
- <sup>4</sup>O. K. C. Tsui, F. K. Lee, B. Zhang, and P. Sheng, *Phys. Rev. E* **69**, 021704 (2004).
- <sup>5</sup>W. M. Gibbons, P. J. Shannon, S. T. Sun, and B. J. Swetlin, *Nature (London)* **351**, 49 (1991).
- <sup>6</sup>M. O'Neill and S. M. Kelly, *J. Phys. D* **33**, R67 (2000).
- <sup>7</sup>K. Ichimura, *Chem. Rev. (Washington, D.C.)* **100**, 1847 (2000).
- <sup>8</sup>E.-K. Lee and J.-H. Kim, *J. Appl. Phys.* **102**, 036102 (2007).
- <sup>9</sup>E.-K. Lee and J.-H. Kim, *J. Phys. D* **41**, 045407 (2008).
- <sup>10</sup><http://www.rsoftdesign.com/>
- <sup>11</sup>H.-S. Kwok, V. G. Chigrinov, H. Takada, and H. Takatsu, *J. Disp. Technol.* **1**, 41 (2005).
- <sup>12</sup>B. Park, Y. Jung, H.-H. Choi, H.-K. Hwang, Y. Kim, S. Lee, S.-H. Jang, M. Kakimoto, and H. Takezoe, *Jpn. J. Appl. Phys., Part 1* **37**, 5663 (1998).
- <sup>13</sup>H. Yokoyama and H. A. van Sprang, *J. Appl. Phys.* **57**, 4520 (1985).
- <sup>14</sup>N. V. Madhusudana and R. Pratibah, *Mol. Cryst. Liq. Cryst.* **89**, 249 (1982).